# Bursting of sensitive polymersomes induced by curling

Elyes Mabrouk, Damien Cuvelier, Françoise Brochard-Wyart, Pierre Nassoy[1], and Min-Hui Li[1]

Institut Curie, Centre National de la Recherche Scientifique, Université Pierre et Marie Curie, Unité Mixte de Recherche 168, Laboratoire Physico-Chimie Curie, 26 rue d'Ulm, F-75248 Paris, France

Edited by Paul M. Chaikin, New York University, New York, NY, and approved March 17, 2009 (received for review December 23, 2008)

**Polymersomes, which are stable and robust vesicles made of block copolymer amphiphiles, are good candidates for drug carriers or micro/nanoreactors. Polymer chemistry enables almost unlimited molecular design of responsive polymersomes whose degradation upon environmental changes has been used for the slow release of active species. Here, we propose a strategy to remotely trigger instantaneous polymersome bursting. We have designed asymmetric polymer vesicles, in which only one leaflet is composed of responsive polymers. In particular, this approach has been successfully achieved by using a UV-sensitive liquid-crystalline copolymer. We study experimentally and theoretically this bursting mechanism and show that it results from a spontaneous curvature of the membrane induced by the remote stimulus. The versatility of this mechanism should broaden the range of applications of polymersomes in fields such as drug delivery, cosmetics and material chemistry.**

asymmetric polymer vesicles | liquid-crystalline copolymer | spontaneous curvature | UV-sensitive

Polymersomes are vesicles made of 10- to 30-nm-thick amphiphilic block copolymer bilayers (1, 2). Compared with liposomes (5-nm bilayer) they are extremely stable and robust, which makes them excellent candidates as drug carriers (3) and microreactors (4). Moreover, targeted transport can be achieved by taking advantage of the many possibilities to end-functionalize the copolymers (5). The controlled release of therapeutic substances can also be integrated through the use of copolymers with blocks that respond to chemical stimuli such as hydrolysis (6, 7), oxidation (8) or reduction (9) reaction, and pH changes (10–17). Common strategies have been to use hydrophobic blocks that can progressively degrade or convert into hydrophilic moieties or to use a cleaveable linkage between hydrophobic and hydrophilic blocks. Upon these chemical stimuli, the vesicular structure is disrupted and the encapsulated substance released within times ranging from seconds to hours. However, in some applications, such as cancer treatment or synthesis of high-value chemicals, a fast and programmed release of entrapped species (drugs, catalysts, or reactants) at a precise site induced by a remote stimulus is desirable to minimize the damage caused by therapeutic agents on the surrounding healthy tissue or to ensure the proper course of the chemical reaction. Although pH- (15, 16) and reduction- (9) responsive systems can respond within seconds or minutes, they require that the chemical environment be modified by additional reagents. These environmental changes may not always be compatible with the drug targeting sites or the chemical reaction conditions. Our strategy is to use a physical stimulus, such as light, leading to a rapid modification of physical structure at the molecular level. We describe a general approach to remotely induce fast bursting of polymersomes (within milliseconds), and we experimentally demonstrate its feasibility using a UV stimulus.

## Results and Discussion

The basic principle to rapidly burst the polymersome is to induce frustration of the polymersome membrane via a remote stimulus. To implement this approach, we prepared asymmetric polymersomes in which each leaflet consisted of a different type of diblock copolymer: One copolymer was insensitive to any remote stimulus whereas the hydrophobic moiety of the second copolymer was a liquid-crystalline (LC) polymer. LC phases are known to respond to magnetic/electric fields, temperature (18), or light (if the mesogen is a chromophore) (19), and LC polymers have been shown to change conformation in response to some of these stimuli (20–22). As an inert copolymer, we selected polyethyleneglycol-*b*-polybutadiene (PEG-*b*-PBD, or PBD for simplicity) (1). The LC-based copolymer, PEG-*b*-PMAazo444 (PAzo), was previously shown to self-assemble into nanopolymersomes (23). The mesogenic unit in the side-on LC block contains an azobenzene group, which undergoes a *trans*-to-*cis* configurational transition upon UV exposure. This isomerization induces a nematic (N) to isotropic (I) transition in the LC polymer (24) causing a conformational change of the chain from a rod to a coil (20, 21). Fig. 1 shows the chemical structures of the 2 selected copolymers and a cartoon of the LC copolymer conformation in the membrane both in the absence and in the presence of UV light. Starting from a thin, cigar-like shape corresponding to N state (23), UV irradiation transforms the LC hydrophobic block to a coil characterized by an increased molecular area. Our initial working hypothesis was that the induced area difference between the 2 polymer monolayers could be sufficient to trigger membrane rupture.

To directly visualize the fate of asymmetric polymersomes under UV illumination, production of giant (more than a few microns in diameter) vesicles was necessary. Classical formation methods such as spontaneous rehydration or electroswelling (1) were precluded because they naturally lead to a symmetric copolymer distribution between both leaflets. Instead, we adapted an alternative method developed by Weitz and coworkers (25) that permits independent assembly of the inner and outer leaflets of the vesicle. Briefly, the inner monolayer is first formed via the emulsification of water droplets in oil containing the first amphiphile of interest. The outer monolayer is then formed by the centrifugation of the water droplets stabilized by the first amphiphile through the monolayer of the second amphiphile at the interface between a second oil solution (containing the second amphiphile of interest) and a water solution (see *Methods*). In contrast to liposomes, the high molecular weight of copolymers should prevent rapid exchange of molecules between the leaflets. Even though direct structural evidence is difficult to obtain, a high degree of asymmetry

Author contributions: E.M., D.C., P.N., and M.-H.L. designed research; E.M. performed research; E.M. and M.-H.L. contributed new reagents/analytic tools; E.M., D.C., and F.B.-W. analyzed data; and F.B.-W., P.N., and M.-H.L. wrote the paper.

The authors declare no conflict of interest.

This article is a PNAS Direct Submission.

[1]To whom correspondence may be addressed at: Laboratoire Physico-Chimie Curie, Centre de Recherche de l'Institut Curie, 26 Rue d'Ulm, F-75248 Paris, France. E-mail: pierre.nassoy@curie.fr or min-hui.li@curie.fr.

This article contains supporting information online at www.pnas.org/cgi/content/full/0813157106/DCSupplemental.

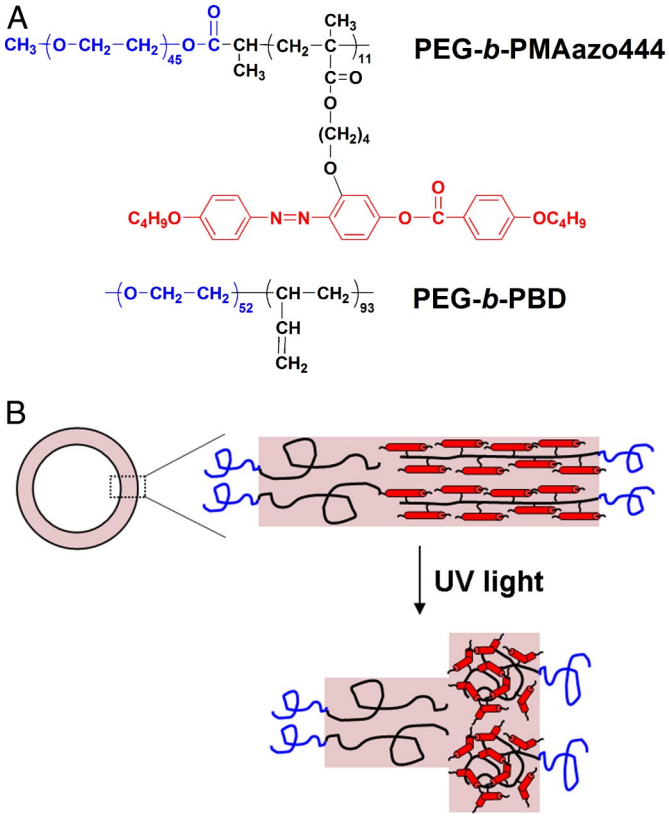


**Fig. 1.** Copolymers and bilayer conformation. (*A*) Chemical structures of the 2 selected copolymers, PEG-*b*-PBD and PEG-*b*-PMAzo444. (*B*) Cartoon of a polymersome and cartoon depicting the conformation of both copolymers within the bilayer for an ePAzo-iPBD vesicle. The PEG-*b*-PBD copolymer is in a coil–coil state. In the absence of UV light, the hydrophobic LC block of the PEG-*b*-PMAzo444 copolymer has a rod-like conformation (corresponding to a nematic state). Under UV illumination, isomerization of the mesogenic groups induces a conformational change of the polymer backbone to a disordered, isotropic state. The net effect of UV exposure is 2-fold: At the molecular scale, the projected area of the LC block is increased; at the mesoscopic scale, the spontaneous curvature of the bilayer is increased.

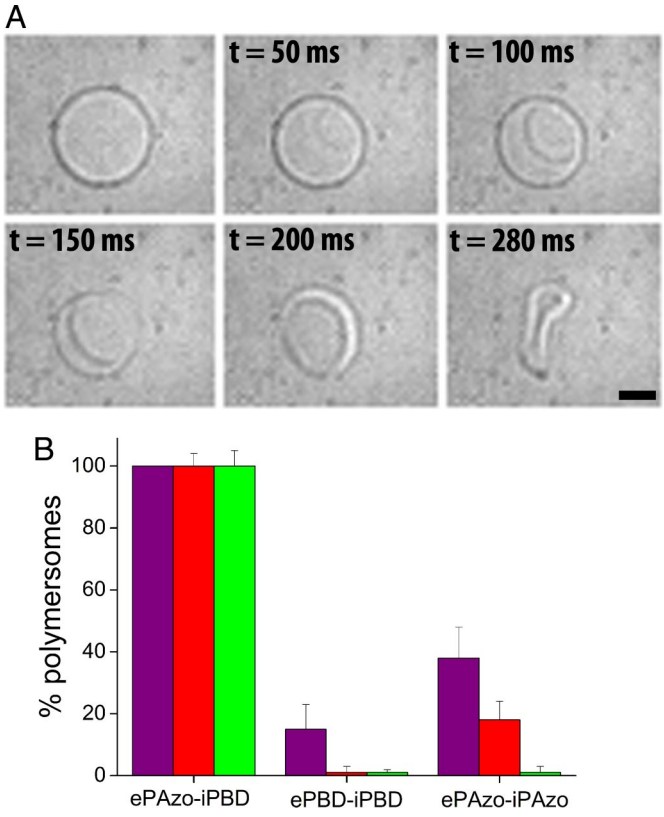


**Fig. 2.** Morphologies of bursting asymmetric polymersomes and statistics of bursting efficiency. (*A*) Snapshots of an ePAzo-iPBD polymersome bursting under UV illumination. Bright-field images were taken by using a high-speed digital camera. The first image shows the vesicle before illumination. Time $t = 0$ corresponds to pore nucleation. The other images show the same vesicle as the pore grows (Scale bar, 5 $\mu$m). (*B*) Fate of polymersomes upon light exposure. Asymmetric ePAzo-iPBD polymersomes and 2 types of symmetric polymersomes (ePBD-iPBD and ePAzo-iPAZo) were tested. Polymersomes were counted as damaged either when the integrity of the membrane was lost or when drastic morphological changes (such as deviation from the initial spherical shape or size) were observed after 5 min of continuous irradiation with a mercury lamp without any specific filter (purple bars) or with UV-irradiation at 360 nm (red bars). Green bars represent the percentage of polymersomes that clearly burst (i.e., total collapse, disappearance or loss of membrane integrity).

between both leaflets is expected and is supported by indirect observations, as shown later.

We first prepared ePAzo-iPBD polymersomes with an external leaflet (e) formed from a PAzo monolayer and internal leaflet (i) obtained by stabilizing a water-in-toluene emulsion with PBD. Fig. 2*A* shows a sequence of images taken with a high-speed camera (10,000 frames per second) of a ePAzo-iPBD polymersome (16 $\mu$m in diameter) exposed to the intense light from a mercury lamp [see also supporting information (SI) Movie S1]. The morphology of the polymersome did not change detectably in the first 30 s before it suddenly burst in <300 ms. As shown in Fig. 2*B*, rapid destruction of all tested polymersomes occurred within the first 5 min of continuous illumination. Similar results were obtained when near-IR light was removed by inserting a UV band-pass filter (360 nm) in the optical pathway, suggesting that vesicles bursting resulted from UV exposure. Control experiments were performed for both types of symmetric polymersomes (ePBD-iPBD and ePAzo-iPAzo). Keeping the illumination time and power constant, the vast majority of ePBD-iPBD vesicles remained intact, and the vesicles that degraded did not burst per se but, instead, underwent slow and partial collapse. This effect was mostly due to local heating because residual degradation of ePBD-iPBD polymersomes could be eliminated by filtering out IR light (Fig. 2*B*). More intriguingly, bursting of ePAzo-iPAzo polymersomes, which are purely composed of UV-responsive material, could not be triggered by UV light. The only apparent effect of UV irradiation on these vesicles was subtle morphological changes such as enhanced membrane fluctuations, and no loss of membrane integrity was evident (Movie S2).

To account for this mechanism of polymersome bursting, we constructed a simple physical model. Vesicles have often been observed to burst upon spreading onto a solid substrate (26), strong aspiration in a micropipette (27), or application of intense electric fields (28). In all these situations, bursting is caused by an increase in membrane tension above the lysis threshold. Clearly, the bursting of these asymmetric vesicles represents a previously uncharacterized phenomenon because, if anything, the light-induced increase of surface area of one of the two leaflets should lead to a decrease in membrane tension. How, then, can bursting be driven by the generation of excess area between both leaflets?

Our proposed mechanism was inspired by a very simple and beautiful classroom experiment that one of us saw when visiting Pierce Hall at Harvard University (Cambridge, MA). As shown in Fig. 3*A*, when a sheet of tracing paper is gently deposited at

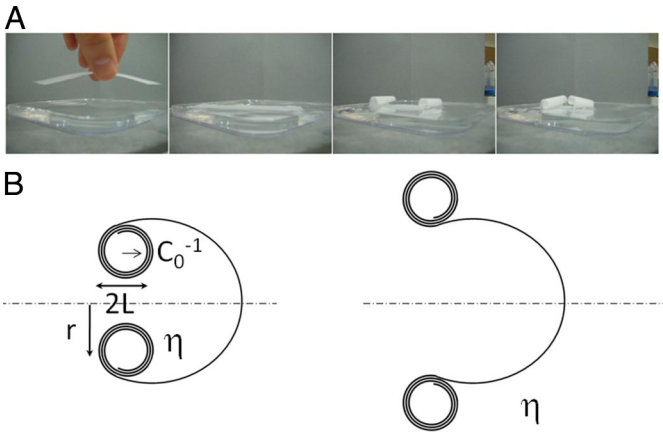


**Fig. 3.** Proposed mechanism for bursting induced by spontaneous curvature. (*A*) Macroscopic classroom experiment showing the curling instability of tracing paper at the water surface. (*B*) Schematic representation of pore opening driven by inward curling (for ePAzo-iPBD, *Left*) or by outward curling (for ePBD-iPAzo, *Right*) and notation for the main parameters used in the theoretical model: $r$ is the radius of the pore, $2L$ is the diameter of the rim, and $\eta$ is the viscosity of the inside (outside) solution when the rim curls inwards (outwards).

the surface of water it undergoes a drastic morphological change. Within a few seconds, both ends curl up and eventually form 2 cylinders of rolled paper. This curling instability is caused by the swelling of the side of the paper in contact with the water. We propose that the growth of a pore in polymersome membranes is driven by the same curling instability. However, in our case, nucleation of a pore is first required to create an edge and thus initiate curling. When the excess area is created in the outer leaflet, curling is expected to be directed inwards, as sketched in Fig. 3*B Left*. The free energy of a hole of radius $r$ in an infinitely thin and flat membrane (polymersome radius, $R_0 \gg r$) is $F = 2\pi r\tau - \pi r^2(S + \sigma)$, where $\tau$ is the line tension that accounts for the energetic penalty in increasing the size of the edge, $S$ is the stored elastic energy per unit area, and $\sigma$ is the membrane tension. Note that, despite the very classical form of $F$, the driving force for pore opening is not only related to surface tension but contains an additional elastic contribution. The parameter $S$ is associated with the increase of the surface asymmetry and can be most simply written as: $S = \frac{1}{2}\kappa c_0^2$ (where $\kappa$ is the bending rigidity of the membrane and $c_0$ its spontaneous curvature). Minimization of $F$ with respect to $r$ defines a nucleation radius $r^* = \tau/(S + \sigma)$ and an energy barrier $U_b + \pi\tau^2/(S + \sigma)$. The formation of the hole is thermally activated (homogeneous nucleation) if $U_b \approx k_BT$ or nucleated on a defect (heterogeneous nucleation) if $U_b \gg k_BT$.

The opening of a pore is accompanied by rapid leaking of the internal liquid, and a concomitant fast relaxation of $\sigma$ (29), which would usually lead to pore healing. Consequently, once the pore is formed, the dynamics of bursting is solely governed by a transfer of surface elastic energy into viscous dissipation of the moving rim formed by membrane curling:

$$2\pi rS\dot{r} = 2\pi r\left(\frac{4\pi}{\ln(2\pi r/L) + 1/2}\right)\eta\dot{r}^2, \qquad [1]$$

where $L$ is the width of the rim, and $\eta$ is the viscosity of the surrounding medium. The term on the right-hand side is the Stokes friction on the moving rim. To first approximation, we assume that the drag coefficient corresponds to a cylinder (of length equal to the perimeter of the pore and of constant radius $L$) moving perpendicularly to its axis. For simplicity, we approximate the slowly varying logarithmic term by a constant, $\ell_n$. Also note that we have neglected the dissipative contribution due to the surface viscosity $\eta_s$ of the polymer bilayer. This assumption holds if $\eta_s < \eta \cdot r$ and is discussed in Eq. **S1** in *SI Text*.

To derive the bursting dynamics $r(t)$, we need to write the elastic energy $S$ as the pore grows. At time $t = 0$ corresponding to pore nucleation, the initial elastic energy is set by the spontaneous curvature $c_0$ associated with the conformational change of the copolymers within 1 leaflet and is given by $S_0 = \frac{1}{2}\kappa c_0^2$. Pore growth enables relaxation of $S$ down to $S = \frac{1}{2}\kappa c^2$, where the curvature of the rim, c, is set by the size of the rim, $c \approx L^{-1}$. From mass conservation: $\pi r^2 e = 2\pi r\,(\pi L^2 - \pi c_0^{-2})$ (with $e$ being the membrane thickness), one finds that the elastic energy $S$ at time $t$ is given by: $1/S = 1/S_0 + (e/\pi\kappa)r$.

By defining a critical pore radius:

$$r_c = \frac{\pi\kappa}{eS_0}, \qquad [2]$$

Eq. **1** reads:

$$\frac{S_0}{1 + r/r_c} = \left(\frac{4\pi}{\ell n}\right)\eta\dot{r}, \qquad [3]$$

and we arrive at:

$$r^2 + 2rr_c = Dt, \qquad [4]$$

where the rate coefficient $D$ (with dimensions of a diffusion constant) is given by:

$$D = \frac{\kappa\ell_n}{2e\eta}. \qquad [5]$$

From Eq. **4**, the dynamics of pore opening $r(t)$ is thus expected to exhibit 2 regimes: (*i*) at short times, $r \approx v^*t$, with $v^* = D/2r_c = S_0\ell_n/4\pi\eta$ being a characteristic velocity, and (*ii*) at longer times, $r^2 \approx Dt$.

We have experimentally monitored the dynamics of pore opening, $r(t)$ (Fig. 4*A*). Two regimes are observed, in agreement with theoretical predictions, and the cross-over occurs at $r_c \approx 6$ $\mu$m. Eq. **2** then provides an estimate of the spontaneous curvature induced by UV illumination, $c_0 \approx 10^{-2}$ nm$^{-1}$. By using typical values for $\kappa \approx 20k_BT$ and $\tau = \kappa/2e \approx 4$ pN (30) (with $e \approx 10$ nm), this value leads to an energy barrier $U_b \approx 10\,k_BT$, which suggests that polymersome bursting is driven by heterogeneous nucleation. We then used Eq. 4 to fit experimental data with only 2 parameters, namely $r_c$ and $D$. For instance, taking $\ell_n \approx 5$, the apparent diffusion coefficient $D$ is predicted to be of the order of 1,000 $\mu$m$^2$·s$^{-1}$ for $\eta = 7 \times \eta_{water}$, which is in good agreement with the value derived from the fit (see Fig. 4*B*). Equivalently, using $c_0 \approx 10^{-2}$ nm$^{-1}$, the slope of the initial linear regime is expected to be of the order of 10 $\mu$m·s$^{-1}$, which is indeed observed experimentally. Furthermore, a critical test of the theoretical picture is the viscosity dependence of the relevant parameters $D$ and $r_c$. Let us recall first that $\eta$ is the viscosity of the medium in which the membrane curls. We varied the viscosity contrast between the interior and the exterior of polymersomes by adding glycerol to the inside solution. In Fig. 4*B*, we plot $D$ and $r_c$ as a function of the relative viscosity $\tilde{\eta} = \eta/\eta_{ref}$ (with $\eta_{ref} = 2.6 \times 10^{-3}$ N·s·m$^{-2}$—see *Methods*). Over the whole range of $\tilde{\eta}$, $r_c$ is found to be constant and equal to $6 \pm 1$ $\mu$m. More importantly, $D$ decreases as $1/\tilde{\eta}$, in agreement with Eq. **5**. Finally, the proposed model of bursting via membrane curling seems to provide a quantitative description of the dynamics of pore opening.

To obtain a direct, model-independent proof for the proposed mechanism, we prepared ePBD-iPAzo polymersomes, which are exactly the reverse configuration of ePAzo-iPBD vesicles. Here,

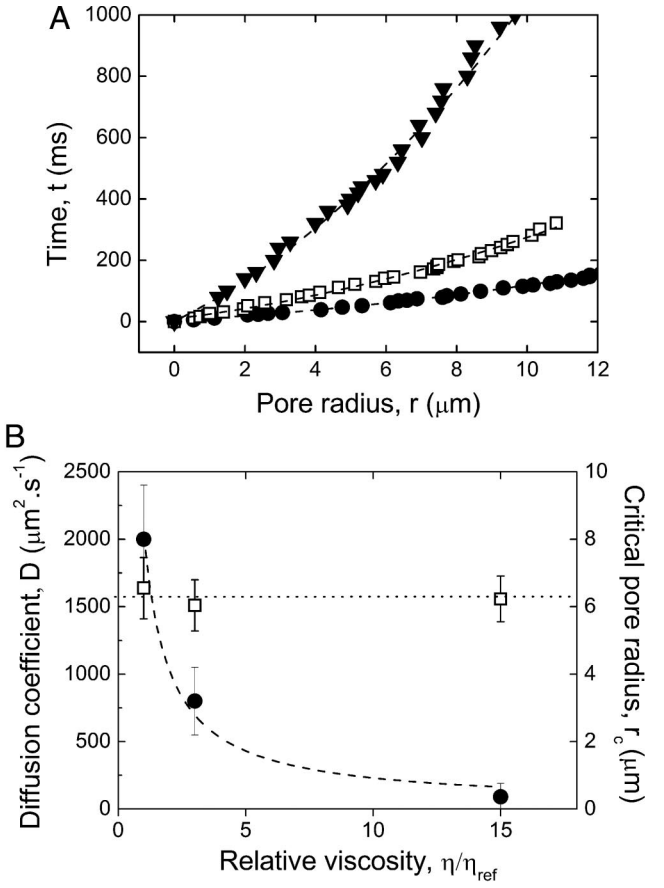


**Fig. 4.** Tests of the theoretical model. (*A*) Dynamics of pore opening: time $t$ as a function of pore radius $r$. Typical curves for 3 different relative viscosities, defined as the viscosity ratio between interior and exterior solutions: (●) $\tilde{\eta} = 1$, (□) $\tilde{\eta} = 3$, (▼) $\tilde{\eta} = 15$. Dashed lines are fits using Eq. **4**. (*B*) Apparent diffusion coefficient $D$ (●) and critical radius $r_c$ (□) as a function of relative viscosity $\tilde{\eta}$. Dashed lines show the predicted dependences, $D \propto 1/\tilde{\eta}$ and $r_c \propto \tilde{\eta}^0$. (*C*) Snapshots of an ePBD-iPAzo polymersome bursting under UV illumination. Bright-field images were taken by using a high-speed digital camera. The first image shows the vesicle before illumination. The image at time $t = 0$ corresponds to pore nucleation, where the image at time $t = 0$ corresponds to pore nucleation and the expulsion of sucrose solution is clearly visible at lower left of the vesicle. The other images correspond to pore growth and clearly show outward spirals (Scale bar, 5 $\mu$m).

the UV-responsive copolymer is restricted to the internal leaflet. As sketched in Fig. 3*B Right*, the change of spontaneous curvature in the inner leaflet is expected to generate an outward curling rim. Exposure to UV illumination caused all ePBD-iPAzo vesicles to burst, and as for the ePAzo-iPBD vesicles, vesicle rupture was completed in less than a few hundreds of milliseconds (Fig. 4*C* and Movie S3). More importantly, as predicted by the theoretical model, the video sequence in Fig. 4*C* clearly reveals that pore opening is accompanied by the formation of an outward curling rim. It is interesting to note that electron micrographs of similar curls or spirals have been observed upon hypotonic lysis of red cell membranes and were interpreted as intermediates for the formation of inside-out vesicles (31).

## Conclusion

These results highlight a general strategy to create stimuli-responsive polymersomes based on the fabrication of asymmetric membranes. For such membranes, polymersome bursting can be driven by a change in membrane spontaneous curvature instead of an increase in membrane tension or a chemical degradation of block copolymers. Although UV light was the stimulus used for this study, temperature or electric or magnetic fields could also act as remote stimuli provided that one of the two leaflets of the membrane is composed of suitably designed LC copolymers. This flexibility, combined with the low permeability of polymer bilayers, ensures a wide range of potential applications in the fields of drug delivery, cosmetics, and material chemistry.

## Methods

**Copolymers and Reagents.** Polyethyleneglycol-*b*-polybutadiene (PEG-*b*-PBD) was purchased from Polymer Source Inc. The diblock copolymer used in this study had a molecular weight of $M_n = 7{,}300$ g·mol$^{-1}$ (by NMR), a polydispersity of $M_w/M_n = 1.06$, and a hydrophilic/hydrophobic weight ratio of 31:69. Polyethyleneglycol-*b*-poly(4-butyloxy-2′-(4-(methacryloyloxy)butyloxy)-4′-(4-butyloxybenzoyloxy)azobenzene) (PEG-*b*-PMAazo444) was synthesized and characterized as described previously (23). The sample chosen had a molecular weight of $M_n = 8400$ g·mol$^{-1}$ (by NMR), a polydispersity of $M_w/M_n = 1.14$, and a hydrophilic/hydrophobic weight ratio of 24:76. All other chemicals (sucrose, glucose, glycerol, dextran, toluene, $\beta$-casein) were purchased from Sigma–Aldrich.

**Preparation of Polymersomes.** All polymer vesicles were obtained by adapting the inverted emulsion method (25). The general protocol, as modified for polymersome formation, is described below. For convenience, the copolymer that will form the outer leaflet of the vesicle is referred to as copolymer (e) and the one used for the inner leaflet is copolymer (i). Two oil phases were prepared by sonicating and dissolving the copolymers (i) and (e) in toluene at 50 °C for 2 h with a typical concentration of 3 mg·ml$^{-1}$. An aqueous solution (referred to as internal buffer) was prepared by adding 100 mg·ml$^{-1}$ dextran ($M_w = 41{,}000$ g·mol$^{-1}$) to a 380 mOsm sucrose-based buffer solution. Note that, although not crucial for polymersome production, dextran was found to significantly improve the protocol efficiency. Five microliters of this internal buffer was added to 500 $\mu$L of the oil phase (i) in a centrifuge tube (Eppendorf). Emulsification was achieved by gentle and repeated pipetting by using a syringe. In parallel, 30 $\mu$L of a 380 mOsm glucose solution (referred to as external buffer) was placed in a centrifuge tube, and 30 $\mu$L of the oil phase (e) was gently layered on top. Because of their amphiphilic nature, some diblock copolymers (e) are expected to diffuse from the oil phase to the interface. Finally, 50 $\mu$L of the water–oil (i) emulsion was transferred to this tube. The tube was immediately centrifuged at 100 × *g* for 12 min (5417R; Eppendorf) so as to avoid any exchange of copolymers between the monolayers. Centrifugation caused accelerated sedimentation of the inverted emulsion droplets through the oil (e)-external buffer interface. A sketch of the protocol is displayed in Fig. S1. Depending on the chemical nature of copolymers (e) and (i), the centrifugation cycles were optimized empirically. Asymmetric ePAzo-iPBD and ePBD-iPAzo polymersomes were centrifuged for 12 min at 100 × *g*, whereas gentler centrifugation was required for symmetric ePAzo-iPAzo polymersomes (10 min at 27 × *g*). In contrast, symmetric ePBD-iPBD polymersomes were less fragile and could be centrifuged successfully for 12 min at 100 × *g*, 8 min at 350 × *g*, and 3 min at 500 × *g*. Finally, for all experiments in which the internal viscosity was increased, the production efficiency was improved by decreasing both the centrifugation speed and duration. Bulk viscosities of all solutions were measured with a capillary viscosimeter (Ubbelohde method). For the aqueous solution of dextran (41,000 g·mol$^{-1}$, at 100 mg·ml$^{-1}$), we found $\eta_{ref} = (2.6 \pm 0.4) \times 10^{-3}$ N·s·m$^{-2}$. We also prepared 45/55

and 70/30 (% vol/vol) glycerol/water solutions, corresponding to viscosities of $(7.7 \pm 0.4) \times 10^{-3}$ and $(39.5 \pm 0.4) \times 10^{-3}$ N·s·m$^{-2}$, respectively.

**Optical Microscopy and UV Illumination.** Sample chambers were built with 2 clean coverslips assembled with a spacer made of Sigillum wax (Vitrex). The chamber was first filled with glucose solution (380 mOsm). A few microliters of the polymersomes suspension was then transferred to the chamber, which was then sealed with mineral oil to prevent water evaporation. The sample was placed on the stage of an inverted microscope (Axiovert 200; Zeiss) equipped with a 100-W mercury lamp (HBO; Osram) and a 40× UApo 340 objective (Olympus) with enhanced transmission for UV excitation. Two kinds of illumination tests were carried out. In the first test, no filter was used, and vesicles were irradiated for a given period (typically 5 min). Polymersomes were imaged before and after exposure. All vesicles that exhibited morphological changes were counted as damaged vesicles, and the disappearance of vesicles was assigned to bursting. In a second test, insertion of a UV band-pass filter (U-360; Edmund Optics, $\lambda_{max} = 360$ nm, FWHM = 45 nm) allowed direct visualization of the polymersomes during light exposure. The intensity of the light coming out of the objective was measured with a power meter (model #70260; Oriel, with UV 70282 silicon probe) and found to be of the order of 1 W·cm$^{-2}$ in presence of the UV filter and of 4 W·cm$^{-2}$ without any filter. Images ($64 \times 64$ pixels) were acquired with a high-speed digital camera (Phantom 4.2; Vision Research) at a rate of 10,000 frames per second.

**Data Analysis.** Illumination tests were performed on ≈30 vesicles of each type, except for symmetric ePAzo-iPAzo that were more difficult to obtain with no defect; only 18 ePAzo-iPAzo polymersomes were investigated. The dynamics of pore opening was monitored by using a semiautomated image analysis procedure to measure pore diameter. Briefly, each image was binarized by applying an appropriate threshold and the edge of the pore then tracked after manually detecting its position for the first image. These routines were run by using ImageJ (freeware).

**ACKNOWLEDGMENTS.** We acknowledge the contribution of Jing Yang, who synthesized the LC block copolymer used in the present work. We thank Karine Guevorkian and Gilman Toombes for critical reading of the manuscript, Patrick Keller for stimulating discussions about LC polymers over recent years, Léa-Laetitia Pontani and Cecile Sykes for fruitful discussions about the inverted emulsion protocol, and Jacques Prost for hearty encouragement. We also thank Pierre-Gilles de Gennes for his enthusiastic support, which encouraged M.-H.L. to pursue this field. This work was supported by the Institut Curie and the Centre National de la Recherche Scientifique.

1. Discher BM, et al. (1999) Polymersomes: Tough vesicles made from diblock copolymers. *Science* 284:1143–1146.
2. Discher DE, Eisenberg A (2002) Polymer vesicles. *Science* 297:967–973.
3. Photos PJ, Bacakova L, Discher B, Bates FS, Discher DE (2003) Polymer vesicles in vivo: Correlations with PEG molecular weight. *J Controlled Release* 90:323–334.
4. Vriezema DM, et al. (2007) Positional assembly of enzymes in polymersome nanoreactors for cascade reactions. *Angew Chem Int Ed* 46:7378–7382.
5. Levine DH, et al. (2008) Polymersomes: A new multi-functional tool for cancer diagnosis and therapy. *Methods*, 46:25–32.
6. Ahmed F, Discher DE (2004) Self-porating polymersomes of PEG–PLA and PEG–PCL: Hydrolysis-triggered controlled release vesicles. *J Control Release* 96:37–53.
7. Ghoroghchian PP, et al. (2006) Bioresorbable vesicles formed through spontaneous self-assembly of amphiphilic poly(ethylene oxide)-*block*-polycaprolactone. *Macromolecules* 39:1673–1675.
8. Napoli A, Valentini M, Tirelli N, Muller M, Hubbell JA (2004) Oxidation-responsive polymeric vesicles. *Nat Mater* 3:183–189.
9. Cerritelli S, Velluto D, Hubbell JA (2007) PEG-SS-PPS: Reduction-sensitive disulfide block copolymer vesicles for intracellular drug delivery. *Biomacromolecules* 8:1966–1972.
10. Liu F, Eisenberg A (2003) Preparation and pH triggered inversion of vesicles from poly(acrylic acid)-block-polystyrene-block-poly(4-vinyl pyridine). *J Am Chem Soc* 125:15059–15064.
11. Geng Y, Ahmed F, Bhasin N, Discher DE (2005) Visualizing worm micelle dynamics and phase transitions of a charged diblock copolymer in water. *J Phys Chem B* 109:3772–3779.
12. Chiu H-C, Lin Y-W, Huang Y-F, Chuang C-K, Chern C-S (2008) Polymer vesicles containing small vesicles within interior aqueous compartments and pH-responsive transmembrane channels. *Angew Chem Int Ed* 47:1875–1878.
13. Lomas H, et al. (2007) Biomimetic pH sensitive polymersomes for efficient DNA encapsulation and delivery. *Adv Mater* 19:4238–4238.
14. Du J, Tang Y, Lewis AL, Armes SP (2005) pH-sensitive vesicles based on a biocompatible zwitterionic diblock copolymer. *J Am Chem Soc* 127:17982–17983.
15. Borchert U, et al. (2006) pH-induced release from P2VP-PEO block copolymer vesicles. *Langmuir* 22:5843–5847.
16. Bellomo EG, Wyrsta MD, Pakstis L, Pochan DJ, Deming TJ (2004) Stimuli-responsive polypeptide vesicles by conformation-specific assembly. *Nat Mater* 3:244–248.
17. Rodriguez-Hernandez J, Lecommandoux S (2005) Reversible inside-out micellization of pH-responsive and water-soluble vesicles based on polypeptide diblock copolymers. *J Am Chem Soc* 127:2026–2027.
18. De Gennes PG, Prost J (1993) in *The Physics of Liquid Crystals* (Oxford Univ Press, New York), 2nd Ed, Chapters 1 and 3.
19. Yu Y, Ikeda T (2004) Alignment modulation of azobenzene-containing liquid crystal systems by photochemical reactions. *J Photochem Photobio C* 5:247–265.
20. Cotton JP, Hardouin F (1997) Chain conformation of Liquid-Crystalline polymers studied by small-angle neutron scattering. *Prog Polym Sci* 22:795–828.
21. Li M-H, Keller P, Li B, Wang X, Brunet M (2003) Light-driven side-on nematic elastomer actuators. *Adv Mater* 15:569–572.
22. Warner M, Terentjev EM (2003) in *Liquid Crystal Elastomers* (Oxford Univ Press, New York), pp 40–50.
23. Yang J, et al. (2006) Formation of polymer vesicles by liquid crystal amphiphilic block copolymers. *Langmuir* 22:7907–7911.
24. Li M-H, Auroy P, Keller P (2000) An azobenzene-containing side-on liquid crystal polymer. *Liq Cryst* 27:1497–1502.
25. Pautot S, Frisken BJ, Weitz DA (2003) Engineering asymmetric vesicles. *Proc Natl Acad Sci USA* 100:10718–10721.
26. Johnson JM, Ha T, Chu S, Boxer SG (2002) Early steps of supported bilayer formation probed by single vesicle fluorescence assays. *Biophys J* 83:3371–3379.
27. Evans E, Heinrich V, Ludwig F, Rawicz W (2003) Dynamic tension spectroscopy and strength of biomembranes. *Biophys J* 85:2342–2350.
28. Aranda-Espinoza H, Bermudez H, Bates FS, Discher DE (2001) Electromechanical limits of polymersomes. *Phys Rev Lett* 87:208301.
29. Sandre O, Moreaux L, Brochard-Wyart F (1999) Dynamics of transient pores in stretched vesicles. *Proc Natl Acad Sci USA* 96:10591–10596.
30. Harbich W, Helfrich W (1979) Alignment and opening of giant lecithin vesicles by electric fields. *Z Naturforsch* 34a:1063–1065.
31. Lew VL, Hockaday A, Freeman CJ, Bookchin RM (1988) Mechanism of spontaneous inside-out vesiculation of red cell membranes. *J Cell Bio* 106:1893–1901.